REMOTE SENSING OF FOREST HEALTH

S. Solberg [a, *], E. Næsset [b], H. Lange [a], O. M. Bollandsås [b]

[a] Norwegian Forest Research Institute, Høgskoleveien 8, 1432 Ås, Norway – (svein.solberg, holger.lange)@skogforsk.no
[b] Agricultural University of Norway, Dep. of Ecology and Natural Resource Management, P.O.Box 5003, 1432 Ås, Norway – (erik.naesset, ole.martin.bollandsas)@ina.nlh.no

KEY WORDS: remote sensing, forest health, canopy, tree crown modelling, chlorophyll, SPOT, laser scanning

ABSTRACT:

Extensive monitoring of forest health in Europe has been carried out for two decades, based mainly on defoliation and discolouration. Together these two variables reflect chlorophyll amounts in the tree crown, i.e. as an indicator of foliar mass, and chlorophyll concentration in the foliage, respectively. In a current project we try to apply remote sensing techniques to estimate canopy chlorophyll mass, being a suitable forest health variable. So far, we limit this to Norway spruce only. LIDAR data here play an important role, together with optical and spectral data, either from survey flights or from satellites. We intend to model relationships between foliar mass and LIDAR data for sample trees, and then scale up this to foliar mass estimates for the entire LIDAR area. Similarly, we try to scale up chlorophyll concentrations in sample trees, by modelling a relationship between sample tree chlorophyll and hyper-spectral data. The estimates of foliar mass and chlorophyll concentrations are then aggregated to every 10x10 m pixel of a SPOT satellite scene which is also covered by airborne data, providing an up-scaled ground truth. If we are successful with this, it might be a starting point for developing a new nationwide forest health monitoring system in Norway.

1. INTRODUCTION

On the global scale forests are threatened by population growth and human activities, including deforestation, air pollution and climate change (Anon. 2001, Kimmins 1997). Climate change is likely to cause increasing forest damage and tree mortality from direct and indirect causes (Martinez-Vilalta 2002, Tenow et al. 1999, Auclair 1993), and in Norway we have noted a number of unusually severe and large-scale damage events during recent years (Solberg 1994, Solheim 2001). There is a need for quantitative information on forest health, and how it varies in space and time. Important here is the need for a quantitative and general health variable integrating across diagnoses, because a global climate change may be manifested by a wide range of different damage types. Forest health monitoring has been run by the European forest monitoring programme UN-ECE/ICP-Forests since 1986, with annual health assessments of 320,000 trees throughout Europe (Anon. 2002a). The core of these surveys is binocular assessments of defoliation and discolouration, which indeed are quantitative and general health variables, and they are also integrating across many diagnoses. Forest damage normally leads to defoliation. For example foliage is typically lost after drought stress, is eaten by insects, or killed by frost. Some damage, however, does not lead to defoliation, but only to reduced concentration of chlorophyll and other pigments, which is another general response to most stress (Carter & Knapp 2001, Young & Britton 1990). In severe cases this is observed as yellowing, and examples of this include fungal diseases on foliage and nutrient deficiency.

However, the limitations of these surveys are that they are subjective, and this has created inconsistent spatial patterns, e.g. between regions (Binns et al. 1986) and countries (Innes et al. 1993, Klap et al. 1997); they have low aerial coverage and focus on single trees rather than areas; and they are lacking the ability to integrate some damage types, such as windthrow and snow breakage. Also, defoliation is well suited to track changes in foliage density within a crown, while it is less suitable for tracking foliar mass reductions in the form of reduced crown size.

The aim of this paper is to describe a project which intends to develop a method for monitoring of forest health by remote sensing. The project is quite new, and hence, this presentation concentrate on presenting the idea; the data; and some preliminary results mainly connected to Lidar data. The basic idea is that variation in forest canopy chlorophyll per ground area is a suitable measure of variation in forest health, and that this quantity can be estimated from remote sensing data, where Lidar data provide foliar mass estimates (or for that matter, synonomously Leaf Area Index (LAI)) and airborne hyper-spectral data provide chlorophyll concentration estimates via spectral signatures. These two variables, which correspond to the commonly used variables defoliation and discolouration, respectively, are combined to determine canopy chlorophyll masses. On a larger spatial scale, satellite images provide data which can be used to gain similar variables. If this is successful, it might form the basis for a routine monitoring of forest health in Norway by remote sensing.

Remote sensing has already demonstrated its ability to provide forest health-relevant data. It is recognized as the key methodology in understanding the (boreal) forest biome and its interactions with the atmosphere, biosphere, and the carbon cycle (Gamon et al. 2004). Some excellent work has been performed to extract key observables such as LAI, fractional cover, dry matter, and water content (Schaepman et al. 2004); chlorophyll (Malenovský 2002, Zarco-Tejada et al. 2004); lignin and nitrogen (Martin & Aber 1997) from remotely sensed data. Even identification of trees infected with root-rot, which is not obviously possible by visual inspection alone, has shown to be feasible (Leckie et al. 2004). Airborne Lidar is recognised as an excellent means for deriving forest parameters of relevance, especially structural parameters such as leaf density, leaf loss and canopy structure (Brandtberg 2003, Lefsky et al. 1999).

Although all these investigations provide corner steps in understanding and interpretation of remote sensing data sets, they are usually confined to one sort of data (i.e., either airborne or satellite-based), very few channels or ratios of spectral coefficients only (for an exception, see Malenovský 2002) and/or mono-aged single-species stands. Our approach differs from that in several aspects:

- Extremely high spatial resolution. Our data allow for the identification of structures well below the single tree scale, and thus tree crowns are not handled in a parametrized way but spatially explicit.

- Collection of very different data types. We combine in our project ground-based assessments on needle, branch, single tree and probe circle with Lidar data from flights, hyperspectral data from an airplane, and satellite images (SPOT and Hyperion). This mixture is a chance and a challenge at the same time.

- The 16 probe circles cover a wide range of age classes, from very young (age class II) to overmature (age class V); in addition, most of the probe circles have a multilayered canopy architecture. Although circles were selected for fair homogeneity, the topography of the site and its character as a natural reserve with absent management make them very diverse even on small spatial scales.

- Full exploitation of hyperspectral information. Rather than relying on well-known indices (e.g. NDVI), we are investigating the measured spectra at all channels, using local as well as integrated properties (Carter and Spiering 2002).

2. MATERIALS AND METHODS

2.1 Study area

The area for this study is located nearby Oslo, south-eastern Norway (59º 50´N, 11º 02´E, 190–370 m a.s.l). The size of the area is 6 km^2, comprising mainly Norway spruce (*Picea abies* L. Karst.) and some Scots pine (*Pinus sylvestris* L.). One large part of the area consists of old forest stands only. This area is a forest reserve, where no clear-cuttings have been executed since 1940 and it is considered as a primeval forest, being partly multi-layered.

2.2 Sample plot inventory

We subjectively selected 16 spruce sites for sample plots, being in the four age-classes with the Norwegian labelling II; III; IV and V with corresponding tree heights in the plots being around 0.5-6; 7-14; 15-20; and 21-35 m, respectively. Ground data were gathered in 2003. We used differential GPS for determining plot coordinates. The planimetric plot coordinates (Euref89) was determined in the center of each plot by means of Global Positioning System (GPS) and Global Navigation Satellite System (GLONASS). A Javad Legacy 20-channel dual-frequency receiver, observing pseudorange and carrier phase of both systems, was used as rover equipment. The receiver setup had a two-second logging rate, and all satellites below a 15º angle from the antenna (cutoff angle) were disregarded. The logging period on each plot ranged between 0.5 and 1.5 hours, with an antenna height of four m. A similar Javad Legacy GPS+GLONASS receiver was established as base station within a distance of <2.5 km from the sample plots. The planimetric coordinates (x and y) of the base station was determined with an accuracy of approximately 0.4 cm. The base

station records were used as reference during post-processing of the rover coordinates. To ensure that the base station received signals from the same satellites as the rover, the cutoff angle was set to 12º. The post-processing of all rover records was undertaken by means of the Pinnacle version 1.0 software package by Topcon (Anon. 1999). The post-processing together with the study by Næsset (2001) indicated an accuracy of the x and y coordinates to be mostly less than one cm, however with one extreme value of 80 cm.

On each plot, the diameter at breast height (dbh) was callipered for all trees with dbh ≥3 cm. Also, for each tree we recorded defoliation, discolouration, polar co-ordinates from the plot center, social status according to Schotte, and tree species. The number of trees on each plot ranged from 76 to 239, with the highest numbers in the younger stands. The total number of trees callipered was 2202.

2.3 Sample tree and sample branch data

On each plot four sample trees of the non-suppressed trees were systematically sampled as sample trees, being the first tree found going clockwise around the plot after each main cardinal direction. On these 64 sample trees were measured height; crown base; and crown width in four cardinal directions. Heights of sample trees were measured by a Vertex III hypsometer. All living branches were callipered and counted in 0.5 cm classes, separately for the lower, middle and upper crown parts (crowns divided in three equally long parts). In the middle of each crown part, four sample branches were cut, - one to each cardinal direction. These sample branches were measured for fresh weight, basal diameter and length. Out of the 12 branches from each tree, 3 + 3 were systematically sampled for further analyses. Three; i.e. one from each crown height, were taken indoors for drying at 65 ˚C, and weighting of the foliar mass. From three other branches, foliage was sampled for chlorophyll analyses, stored at low temperature in the field and during transport to the laboratory.

2.4 Airborne laser scanner data

A Hughes 500 helicopter carried the ALTM 1233 laser scanning system produced by Optech, Canada. The laser scanner data were acquired the 9th of October 2003. The leaf conditions were in an intermediate state, i.e the deciduous trees were still foliferous. The average flying altitude was approximately 600 m above the ground with an average speed of 35 ms^{-1}. 21 flightlines were flown with an overlap between adjacent stripes of about 20 %. Approximately 37 million pulses were transmitted. The pulse repetition frequency was 10 kHz and the scan frequency was 50 Hz. Maximum scan angle was 11°, which corresponded to an average swath width of about 230 m. Pulses transmitted at scan angles that exceeded 10.5° were excluded from the final dataset. The average footprint diameter for individual plots was approximately 18 cm. The mean number of pulses transmitted was 5.0 per m^2. First and last returns were recorded.

The operating firm, Blom Norkart Mapping AS, Norway, undertook a complete post-processing of the first and last pulse data. Planimetric coordinates (x and y) and ellipsoidic height values were computed for all first and last returns. The last return data were used to model the terrain surface. In a filtering operation on the last return data undertaken by the operating firm using a proprietary routine, local maxima assumed to represent vegetation hits were discarded. A triangulated irregular network (TIN) was generated from the planimetric coordinates and corresponding height values of the individual

terrain ground points retained in the last pulse dataset. The ellipsoidic height accuracy of the TIN models was expected to be around 20-30 cm (Kraus & Pfeifer 1998, Reutebuch et al. 2003, Hodgson & Bresnahan 2004). All first and last return observations (points) were spatially registered to the TIN according to their coordinates. Terrain surface height values were computed for each point by linear interpolation from the TIN. The relative height of each point was computed as the difference between their and the terrain surface height.

2.5 Airborne hyper-spectral data

We used a newly developed instrument, the ASI (Airborne Spectral Imager developed by NEO Anon. 2004). The instrument is a pushbroom scanner that covers the spectral region 400 to 1000 nm (VNIR) with a spectral sampling interval of 3.7 nm. It is normally mounted in an aircraft like Cessna 172, where GPS and inertial navigation system data are logged continuously to provide geometric correction and geo-referencing of the images. It is based on the results of the HISS (Hyperspectral Imager for Small Satellites) definition study performed by NEO for ESA in 1996-97.

2.6 Satellite data

We have two SPOT quarter-scenes and one hyper-spectral image (Hyperion) covering the area from the same summer and autumn 2003. These are currently being pre-processed.

2.7 Foliar mass and Lidar

We develop relationships between ground measurements of foliar mass and defoliation and laser data from airborne LIDAR. Laser has the ability to penetrate the vegetation and provide a 3-d dataset of biomass above ground, which is closely related to the amount of foliage, i.e. to foliar mass, crown density and LAI.

2.8 Tree detection and positioning

For correcting possible GPS offsets between the ground and airborne georeferencing, positions of single trees in the Lidar data set was done by finding local maxima in the digital canopy model (DCM) This was done using SURFER software (Anon. 2002b), by firstly setting up a grid of 10 x10 cm over the sample plots and assigning a z-value for each grid node being the maximum z-value of the first returns within a circle of 50 cm radius around each node. Secondly, the DCM was created by fitting these z-values to a "minimum curvature" surface model. This surface was 'polished' running a 3x3 gaussian filter 10-20 times.
Trees were then identified as local maxima in this surface, i.e. grid nodes being higher than their nearest eight neighbours. Compared to the positions of trees in Schotte's social status classes 1-3 in the ground truth, this gave: n trees were not found, nn non-existing trees were 'found', and nnn trees were identified as two or more trees. Some of the latter ones were trees with twin tops or top breakage.

2.9 The chlorophyll and the final up-scaling

The previous point is widened up using airborne hyper-spectral data to model chlorophyll concentrations measured in the forest canopy layer, which together with the foliar mass data provides canopy chlorophyll data, integrating any type of forest damage (at least at a developed stage where symptoms are observable). To that end, we establish a relationship between direct

chlorophyll content measurements on needles for selected trees and properties of the individual spectra, such as the NDVI, the first oder derivative green vegetation index (Elvidge and Chen 1995), or the green normalized difference vegetation index (Gitelson and Merzlyak 1998). When exploiting the full set of (160) channels available from the hyperspectral images (contrary to the SPOT images), we calculate wavelength-dependent canopy reflectance (normalized to standardized). We intend to use the empirical models between foliar mass and Lidar, and between chlorophyll concentrations and hyper-spectral data for up-scaling of the ground truth to every pixel in the satellite scenes, i.e. to a reference wavelength (e.g. 820 nm)) versus chlorophyll content correlations 10x10 and 30x30 m pixels, and to determine maximum sensitivity. It has been shown (Carter and Spiering 2002) that this usually leads to maximum correlation coefficient of 0.9 and above.

2.10 Handling of shadowing and edges

The interpretation of individual pixels from satellite images crucially depends on available information on illumination (sun elevation, cloud cover), viewing angle, and obstructions by objects outside the pixel. It has been shown that shadow fraction and even brightness within the shadow, or radiation load, crucially determines vegetation properties such as Leaf Area Index (Seed and King 2003) or canopy chlorophyll content (Zarco-Tejada et al. 2004). Thus, radiometric corrections have to be applied, which is done through radiative transfer models. Given the detailed information we have on local topography from Lidar and on satellite position, we proceed to correct for shadowing and obstacles as follows. First we calculate an imaginary solar path length, and use the Lidar DEM to calculate subpixel areas in the shadow using raytracing algorithms (Jones 1997). Secondly, each image pixel (10 m x 10 m) is assigned a "shadow fraction" counting the number of subpixels contained which are in the shadow. This matrix is then multiplied with the direct beam radiation map calculated from the satellite's position. Finally, a viewshed (Dozier and Frew 1990) function customary in numerous radiation models is applied to each pixel. The resulting pixel matrix can then be investigated in a quality assessment step to exclude pixels highly influenced by shadowing from further analysis, e.g. by assigning a threshold (e.g. of 50%) to convert the shadow fraction map into a binary shadow matrix prior to multiplication with the direct beam radiation map.

3. PRELIMINARY RESULTS AND DISCUSSION

3.1 Ground data: Branch, foliage and chlorophyll data

Branch fresh weights were strongly correlated to branch basal area. A linear regression for branch weight (g) against branch basal area (mm^2) with R^2=0.82 had the following equation:

[1] Branch fresh weight = -47 + 3.1 * branch basal area

Using this model together with the branch counts gave total branch weights of the sample trees ranging from 4 to 740 kg, with averages given in Table 1. On average 23% of the branch fresh weight was made up by needle dry weight. Concentration of total chlorophyll (chl a + chl b) was on average 1.1 mg/g needle fresh weight. Given 65% water content of the needles, the chl concentration was 3.1. mg/g needle dry weight. An overview of some average tree and branch data is given in table.

1. These estimates will be refined using more explanatory variables at hand; i.e. canopy level, cardinal direction and branch length.

Table 1. Mean tree diameter; height; branch weight, foliar mass and chlorophyll mass, all by age class

Age class	D Mm	H m	Branch fw kg	Foliar dw kg	Chl g
II	50 [1]	4	18	4	12
III	79	9	64	15	47
IV	172	21	287	66	205
V	189	20	412	95	295

[1] diameter in age class II measured at the ground

3.2 Canopy surface

The minimum curvature surface worked well in the sense that very few Lidar residuals had a positive sign; i.e. z-values above the surface (about 4%). And it followed smoothly the uppermost Lidar observations (Fig. 1). Only in the border areas between trees and treeless openings it tended to overestimate the canopy surface height. This requires further refinement.
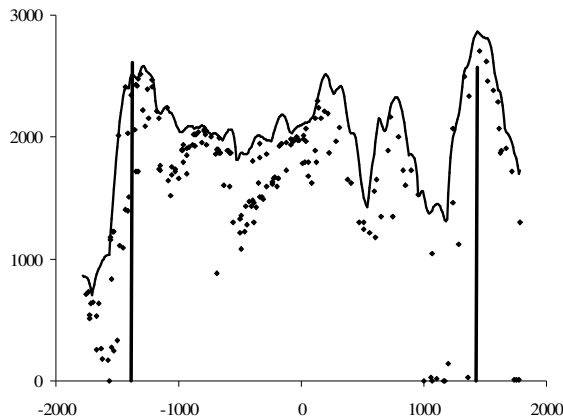

Fig. 1. DCM: First Lidar returns and mean canopy surface in a one m wide belt across plot 1 (old spruce forest) after using a minimum curvature model. The stem of two trees are included, - their positions and heights from ground measurements. Scale unit = cm.

3.3 Tree detection and positioning

When comparing the positions of ground measurements and the Lidar data, we found indications of an offset between them. Local maxima in the Lidar data tended to be about one m to the northwest compared to the positions of tree stems as measured from the ground (Fig. 2). The differences in positions varied, which is to be expected due to some trees with double tops, trees with not vertical stems, and trees with top-breakage. However, there is a clear tendency throughout this plot of an offset. A similar offset was found in plot 1, and we continue to check this for other plots.
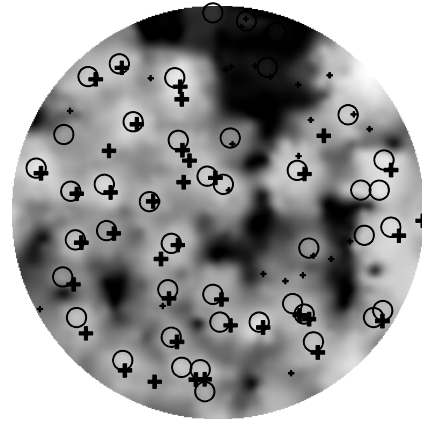

Fig. 2. Offset in plot 4 (old forest): Lidar local maxima (O), and positions of trees in social status 1 and 2 (+) and social status 3 and 4 (+) as measured from ground using differential GPS.

3.4 Lidar data and foliar mass

In order to correlate Lidar data to foliar mass, the Lidar data had to be assigned to the trees, and this was done by estimating crown projections in the horizontal plane. As a starting point this was done by developing a crown model as follows. Firstly, the crown widths were modelled as a linear function of tree diameter, using only crown widths that were classified as not influenced by competition. A grid of 10x10 cm were put over the sample plot, and all trees made a claim for every grid node within their estimated crown width, where the claim was proportional to the tree height and decreasing linearly from the stem centre outwards and reaching zero at the outline of the projection. Every grid node was then assigned to that tree having the highest claim. An example from plot 1, age class V (old stand) is given in Fig. 3.
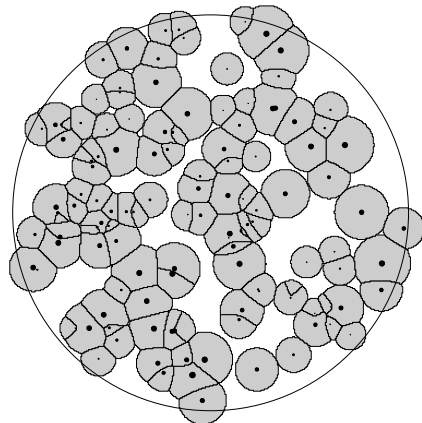

Fig. 3. Tree crown projections in plot 1 (old forest), as estimated by a theoretical "claim" model (see text for details).

From this the crown projection area was calculated for every tree. As a measure of foliar density, a Lidar index was calculated for each tree, as the fraction of first returns that did not hit the ground, i.e. its z-value were at least 10% of the tree height. For the 64 sample trees a regression of foliar dry mass (kg) against crown projection area (m^2) and the Lidar index came out as follows:

Foliar mass = -13 + 8.9*Lidar_index + 5.7*crown_area ,

with R^2=0.82 and both coefficients for the explanatory variables being significantly different from zero. However, the crown area had a much stronger influence on the foliar mass than the Lidar index. This is likely due to have three explanations. Firstly, most trees were fairly healthy with fairly dense canopies. Thus, the ability of a Lidar pulse to penetrate the entire crown and hit the ground did not differ strongly between the trees. Secondly, the crown projections were preliminary, and needs to be refined considerably. The offset that was likely present between the GPS positioning made from ground and in the flight was not adjusted for. Finally, the suppressed trees were not taken into account, although their stems and branches were often present under the sample tree crowns.

The high density Lidar data appears to be a promising tool for foliar mass or defoliation measurements (Fig. 4).
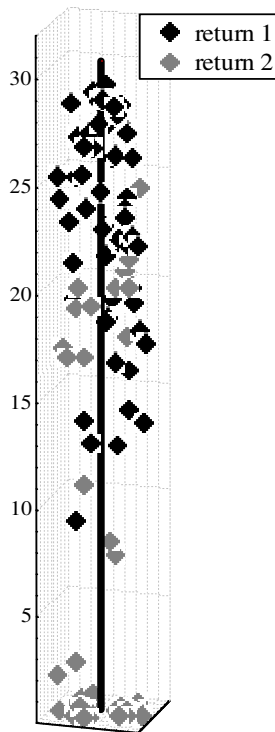

Fig. 4. Lidar data assigned to tree nr 27 on plot 1, as well as the stem position and height as measured at the ground.

4. CONCLUSIONS

We believe remote sensing is a promising tool for future forest health monitoring, in particular when combining Lidar and hyper-spectral data-sources. The high density Lidar data appears to be a suitable tool for foliar mass or defoliation measurements. This and other preliminary results indicate this, although considerable work remains to be done in order to eventually realize this.

REFERENCES

Anon. 1999. Pinnacle user's manual, Javad Positioning Systems, San Jose, CA, pp. 1-123.

Anon. 2001. IPCC (The Intergovernmental Panel on Climate Change). Climate Change 2001: Impacts, Adaptation and Vulnerability. http://www.ipcc.ch (Accessed 15. June 2004)

Anon. 2002a. UN/ECE & EC. / Lorenz, M., Mues, V., Becher, G., Müller-Edzards, Ch., Luyssaert, S., Raitio, H., Fürst, A., Langouche, D. Forest Condition in Europe - 2003 Technical Report, Geneva, Brussels

Anon. 2002b. *Surfer. User's guide.* Golden software inc., Golden, Colorado, pp. 1-640.

Anon. 2004. ASI – Airborne spectral imager. NEO (Norwegian electro optics) http://www.neo.no/asi (accessed 14. Aug. 2004)

Auclair, A.N.D., Worrest, R.C., Lachance, D. & Martin, H.C. 1993. in: Manion, P.D. & Lachance, D. (Eds) APS press. The American Phytopathological Society. St. Paul, Minnesota. 249 pp.

Binns, W.O., Redfern, D.B., Boswell, R. & Betts A.J.A. 1986. Forest health and air pollution. 1985 survey. Forestry commision research and development paper 147: 1-16.

Brandtberg, T., Warner, T., Landenberger, R. and McGraw, J., 2003, Detection and Analysis of Individual Leaf-off Tree Crowns in Small Footprint, High Sampling Density Lidar Data from the Eastern Deciduous Forest in North America, Remote Sensing of Environment, vol. 85, no. 3, pages 290-303.

Carter, G. & Knapp, A.K. 2001. Leaf optical properties in higher plants: Linking spectral characteristics to stress and chlorophyll concentration. American Journal Of Botany 88: 677-684.

Carter, G.A., and B.A. Spiering (2002). Optical properties of intact leave for estimating chlorophyll concentration. J. Environ. Qual. 31,1424-1432.

Dozier, J. and Frew, J. (1990): Rapid calculation of terrain parameters for radiation modeling from digital elevation model data. IEEE Transactions on Geoscience and Remote Sensing, 28:963-969

Elvidge, C.D., and Z. Chen (1995): Comparison of broad-band and narrow-band red and near-infraredvegetation indices. Remote Sensing of Environment 54, 38-48.

Gamon, J. A., Huemmrich, K. F., Peddle, D. R., Chen, J., Fuentes, D., Hall, F. G., Kimball, J. S., Goetz, S., Gu, J., McDonald, K. C. 2004. Remote sensing in BOREAS: Lessons learned. Remote Sensing of Environment. 89(2): 139-162.

Gitelson, A.A., and M.N. Merzlyak (1998): Remote sensing of chlorophyll concentration in higher plant leaves. Advances in Space Research 22, 689-692.

Hodgson, M. & Bresnahan, P. 2004. Accuracy of airborne lidar-derived elevation: empirical assessment and error budget. Photogramm. Eng. Remote Sensing, 70:331-339.

Innes, J.L., Landmann, G. & Mettendorf, B. 1993. Consistency of observations of defoliation amongst three different European countries. Environmental Monitoring and Assessment 25: 29-40.

Jones, M.W. (1997): An Efficient Shadow Detection Algorithm and the Direct Surface Rendering Volume Visualisation Model. In: Proc. 15th Ann. Conf. of Eurographics (UK Chapter), 237-244.

Kimmins, J.P. 1997. Forest ecology: a foundation for sustainable management. Prentice Hall, New Jersey. Pp. 1-596.

Klap, J., Voshaar, J.O., De Vries, W. & Erisman, J.W. 1997. Relationships between crown condition and stress factors. P. 277-301 In: Müller-Edzards, C., De Vries, W. & Erisman, J.W. (Eds) Ten Years Of Monitoring Forest Condition in Europe. Studies on Temporal Development, Spatial Distribution and Impacts of Natural and Anthropogenic Stress Factors. UN-ECE/EC. Brussels, Geneva. 386 pp.

Kraus, K. & Pfeifer, N. 1998. Determination of terrain models in wooded areas with airborne laser skanner data. ISPRS J. Photogramm. Remote Sens., 53:193–203.

Leckie, D.G., Jay, C., Gougeon, F.A., Sturrock, R.N. and Paradine, D. (2004): Detection and assessment of trees with Phellinus weirii (laminated root rot) using high resolution multi-spectral imagery. International Journal of Remote Sensing 25, 793-818.

Lefsky, M., Cohen, W., Acker, S., Parker, G., Spies, T. and Harding, D., 1999, Lidar Remote Sensing of the Canopy Structure and Biophysical Properties of Douglas-Fir Western Hemlock Forests, Remote Sensing of Environment, vol. 70, no. 3, pages 339-361.

Malenovský 2002. Investigation of functional parts and status of Norway spruce crowns using spectral remote sensing information. Thesis Report GIRS 25. Lab of Geo-Inf Science and Rem Sens, Wageningen Univ, pp. 1-74

Martin, M.E. & Aber, J. D. 1997. High spectral resolution remote sensing of forest canopy lignin, nitrogen, and ecosystem processes. Ecological Applications 7: 431-443.

Martinez-Vilalta J, Pinol J, Beven K. 2002. A hydraulic model to predict drought-induced mortality in woody plants: an application to climate change in the Mediterranean. Ecological Modelling 155 (2-3): 127-147.

Næsset E. 2001. Effects of Differential Single- and Dual-Frequency GPS and GLONASS Observations on Point Accuracy under Forest Canopies. Photogramm. Eng. Remote Sensing, 67(9):1021–1027.

Reutebuch, S. E., McGaughey, R. L., Andersen, H. –E. & Carson, W. W. 2003. Accuracy of a high-resolution lidar terrain model under a conifer forest canopy. Can. J. Remote Sensing,, 29:527–535.

Schaepman, M.E., Koetz, B., Schaepman-Strub, G., Zimmermann, N.E. & Itten, K.I. 2004. Quantitative retrieval of biogeophysical characteristics using imaging spectroscopy: a mountain forest case study Community Ecology. In press.

Seed, E.D. and King, D.J. (2003): Shadow brightness and shadow fraction relations with effective leaf area index: importance of canopy closure and view angle in mixedwood boreal forest. Canadian Journal of Remote Sensing 29 (3), 324-335.

Solberg, S.; Solheim, H.; Venn, K.; Aamlid, D. 1994. Tilfeller av skogskader i Norge i 1992 og 1993. Cases of forest damage in Norway 1992 and 1993. Reseach Paper of Skogforsk. 24/94, 1-35

Solheim, H. 2001. Mye brun furu i Sørøst-Norge i år. In: Woxholtt, S. (ed). Kontaktkonferansen mellom skogbruket og skogforskningen i Telemark og Aust-Agder. Drangedal 19. – 21. september 2001. Aktuelt fra Skogforskningen 6/01: 9-11.

Tenow O, Nilssen AC, Holmgren B, Elverum F. 1999. An insect (Argyresthia retinella, Lep., Yponomeutidae) outbreak in northern birch forests, released by climatic changes? Journal Of Applied Ecology 36 (1): 111-122.

Young, A. & Britton, G. 1990. Carotenoids and Stress. p 87-112 In: Alscher, R.G. & Cumming, J.R. (Eds.) Stress responses in plants: Adaptation and acclimation mechanisms. Plant Biology 12. Wiley-Liss. New York. 407 pp.

Zarco-Tejada, P.J., Miller, J.R., Morales, A., Berjón, A. and Agüera, J. (2004): Hyperspectral indices and model simulation for chlorophyll estimation in open-canopy tree crops. Remote Sensing of Environment 90, 463-476.

ACKNOWLEDGEMENTS